Journal of
Ceramic Science
and Technology

*J. Ceram. Sci. Technol.*, **09** [2] 149-154 (2018)
DOI: 10.4416/JCST2017-00089
available online at: http://www.ceramic-science.com


# Electrical and Dielectric Properties of Isostatically Pressed Alumina-Based Electroporcelain

**V. Trnovcová[1], M. Kubliha[2], I. Štubňa[1], Š. Csáki[*1, 3]**

[1]Department of Physics, Constantine the Philosopher University, A. Hlinku 1, SK-94974 Nitra, Slovakia
[2]Institute of Materials, Faculty of Materials Science and Technology,
Slovak University of Technology, J. Bottu 25, 917 24 Trnava, Slovakia
[3]Charles University, Department of Physics of Materials, Ke Karlovu 5, 12116, Prague, Czech Republic
received November 15, 2017; received in revised form January 03, 2018; accepted February 07, 2018

**Abstract**

**The anisotropy of dc and ac conductivities and relative permittivity is studied in green, dehydroxylated, and fired, cold-isostatically pressed alumina-based electroporcelain. The dc conductivity, $\sigma_{dc}$, of green samples is isotropic and its temperature dependence contains two Arrhenius-like sections: below 140 °C, $\sigma_{dc} = 5 \cdot 10^{-2} \exp(-0.77/kT)$, and from 150 to 400 °C, $\sigma_{dc} = 4 \cdot 10^{-4} \exp(-0.56/kT)$, where $\sigma_{dc}$ is in S/cm and conduction activation energies are in eV. The dc conductivity of dehydroxylated samples is also isotropic but much lower: below 200 °C, $\sigma_{dc} = 1.7 \cdot 10^{-3} \exp(-0.8/kT)$; above 210 °C, $\sigma_{dc} = 0.7 \exp(-1.07/kT)$. Fired samples behave as fast-ionic conductors, above 300°C; temperature dependences of both dc and ac conductivities, in both directions, are given as $\sigma = 17 \exp(-0.785/kT)$. The anisotropy of the ac conductivity and permittivity is distinct only in as-received samples, being higher in the samples with a rotational axis in the direction of the blank radius. In green samples, anisotropy of the ac conductivity and permittivity is observed owing to relaxation of water molecules in closed pores and capillaries. The static relative permittivity of dehydroxylated and fired samples is equal to 6.3 ± 0.3 or 6.9 ± 0.1, respectively.**

*Keywords: Electrical conductivity, dielectric properties, alumina-based electroporcelain, cold isostatic pressing*

## I. Introduction

Industrial ceramics are usually treated as isotropic. However, anisometric crystals (especially thin hexagonal platelets of kaolinite), pores, and capillaries can be spatially arranged as a result of some preparation methods. In vacuum extrusion, owing to non-Newtonian velocity profile, the shear forces result in an orientation of anisometric crystals. Thus, a technological texture arises near solid surfaces of large green bulks[1–5]. The technological texture brings about anisotropy of physical properties[6–10]. The texture usually has an unfavorable influence on the performance of ceramics, so it is necessary to detect it with simple methods, before heating the raw bodies.

In this paper, the anisotropy of physical properties of cold-isostatically pressed alumina-based electroporcelain, used for manufacturing large high-voltage insulators, is studied. The alumina-based porcelain has high mechanical strength[11] which is, together with good insulating properties at low temperatures, a very important property of these insulators. The content of alumina in porcelain is a principal factor influencing its mechanical strength[12].

The aim of this work is to study electrical and dielectric properties of as-received, dehydroxylated, and fired isostatically cold-pressed alumina-based electroporcelain, the anisotropy of these properties, and the kinetics of the release of physically (PBW) and chemically (CBW) bound water, and also the influence of this release on the electrical and dielectric properties. Understanding the conduction behavior of green porcelain mixtures at higher temperatures enables more accurate control of furnace temperature during flash sintering, which is an energy-saving modern method of ceramic production[13,14]. The action of technological texture is very unfavorable in large raw insulators as it causes their cracking during firing. Thus, the development of simple methods for detection of technological texture, e.g. for quality control, and development of preparation procedures for producing non-textured large raw ceramic bodies are needed. Moreover, information on the electrical conductivity of the electroporcelain bodies is important because ceramic bodies produced from this porcelain are used as high-voltage insulators.

## II. Material and Methods

The ceramic raw mixture contains 30 mass% kaolin and clay, 30 mass% feldspar, 25 mass% alumina (corundum), and 15 mass% grog (Table 1). A blank disk with a diameter of 120mm is made by means of cold isostatic pressing of the powder obtained from a water suspension of these components (after spray drying), at room temperature (RT), under a pressure of 125 MPa. Cylindrical samples (containing 1mass% PBW) with a diameter of 10mm and thickness

* Corresponding author: stefan.csaki@ukf.sk

**Table 1:** Chemical compositions [in mass%] of raw materials.

| | $SiO_2$ | $Al_2O_3$ | $K_2O$ | $Na_2O$ | Fe, Mg, Ca, Ti oxides | LOI |
|---|---|---|---|---|---|---|
| Kaolin | 53.3 | 31.9 | 0.9 | 0.3 | 1.9 | 11.7 |
| Clay | 50.8 | 31.5 | 0.8 | 0.2 | 5.2 | 11.5 |
| Feldspar | 72.9 | 15.2 | 4.6 | 4.4 | 1.1 | 1.0 |
| Corundum | - | ~100 | - | - | - | - |
| Grog | 52.3 | 40.8 | 0.7 | 0.5 | 4.9 | 0.8 |

of 2 mm are cut from the surface layer of the cylindrical blank where the technological texture is most pronounced[1]. Two kinds of samples are prepared: 1) samples, with a rotational axis, identical with the direction of the electrical field, in direction of the blank radius, denoted "R-samples", and 2) samples, with a rotational axis, identical with the direction of the electrical field, parallel to the blank axis, denoted "A-samples".

The technological texture is studied with X-ray diffraction at RT (powder diffractometer Philips, $CuK_\alpha$ radiation, diffraction angle, $2\theta$, ranging from 5° up to 35°) of both R-samples and A-samples. The texture is studied in as-received samples, in samples heated to 600 °C, with a heating rate of 2 °C/min, and in samples fired at 1430 °C, for 30min. The basic reflection (101) of quartz, or its fainter reflection at 10.6°, is used as an internal standard.

Before electrical measurements, colloidal graphite electrodes are deposited onto both bases of the cylindrical samples and, afterwards, the electrodes are dried under an infrared bulb. Temperature dependences of the dc conductivity are measured with a dynamic electrometer RFT, VA-J-51, in a vacuum of 0.1Pa, at a heating rate of 2 °C/min. Temperature dependences of the ac conductivity and capacitance of the samples are measured in a vacuum of 0.1Pa, at a heating rate of 2 °C/min, using a precise semi-automatic ac bridge Tesla BM 484, at a frequency of 1592Hz, and heating rate of 2 °C/min. Isothermal frequency dependences of the ac conductivity and effective permittivity (calculated from the capacitance and dimensions of samples) are measured both with the dielectric constant and loss factor testing set TR 9701, Orion Budapest, at 0.5 – 100kHz, in $N_2$, and with the impedance meter GB11a, Radiometer, Copenhagen, at 25Hz – 100 kHz, in a vacuum of 0.1Pa. (The atmosphere used has no influence on the results.) For the isothermal measurements of the frequency dependences of the ac conductivity and effective relative permittivity, samples are put in a furnace pre-heated to the chosen temperature. For the ac electrical measurements, the temperature ranges from 20 °C up to 600 °C; for the dc electrical measurements, the temperature ranges from liquid nitrogen temperature up to 600 °C.

Electrical and dielectric properties are measured for as-received samples, after a partial removal of the PBW, then, upon successive heating up to 160, 200, 300, and 400 °C with a rate of 2 °C/min (upon heating, the temperature is stabilized for 10min, free cooling to RT follows, and a measurement of the dc conductivity begins), then during and after releasing the CBW, upon heating to 500, 530, and 600 °C[15], and finally, after firing at 1430 °C for 30min. Impedance or modular analysis is used to determine the bulk dc conductivity and static relative permittivity from the frequency dependences of the ac conductivity and relative permittivity at a constant temperature[6,16]. Modular and impedance diagrams are formed by suppressed circular arcs with centers below the horizontal axis; the bulk resistance and reciprocal static relative permittivity are given by intersections of the arcs with the horizontal axis. Static relative permittivity at room temperature (RT) is determined only for the dehydroxylated and fired ceramics. To reduce the effect of different initial PBW content in various samples, all samples were dried at 110 °C for 4h, before electrical measurements[6,17].

## III. Results

### *(1) X-ray phase analysis*

Green samples of the alumina-based insulating porcelain contain kaolin, feldspar, free corundum, free crystalline quartz, some cristobalite, and traces of mullite (Fig.1a, Table 1). Cristobalite and mullite come from the grog. On cold isostatic pressing, intensity ratios of kaolinite or feldspar (anisometric crystals) diffraction peaks to basic quartz (isometric crystal) diffractions are independent of the orientation of samples. It means that the technological texture resulting from a preferential orientation of these anisometric particles is not formed as a result of this type of pressing[6]. However, a preferential orientation of pores and capillaries, which are XRD-invisible, cannot be excluded.

During dehydroxylation, XRD peaks of kaolinite get smaller and gradually disappear. Other diffraction peaks get higher and narrower; this indicates that during dehydroxylation other crystallites get larger[18]. At 600 °C, the dehydroxylation process is finished (Fig.1b). Kaolinite crystals are transformed to XRD-amorphous metakaolinite particles with a loss of structural hydroxyl groups[19]. However, the morphology of the particles is not substantially changed[19,20]. Metakaolinite particles have the same shape and size as kaolinite crystals, they are only slightly thinner[18]. Therefore, no technological texture is formed and no anisotropy in X-ray plots is observed due to this thermal treatment. Metakaolinite particles have a disordered structure; only a short-range arrangement is preserved in them.

Fired ceramics are isotropic; they contain a glassy phase, corundum, and mullite crystals[21] (Fig.1c).

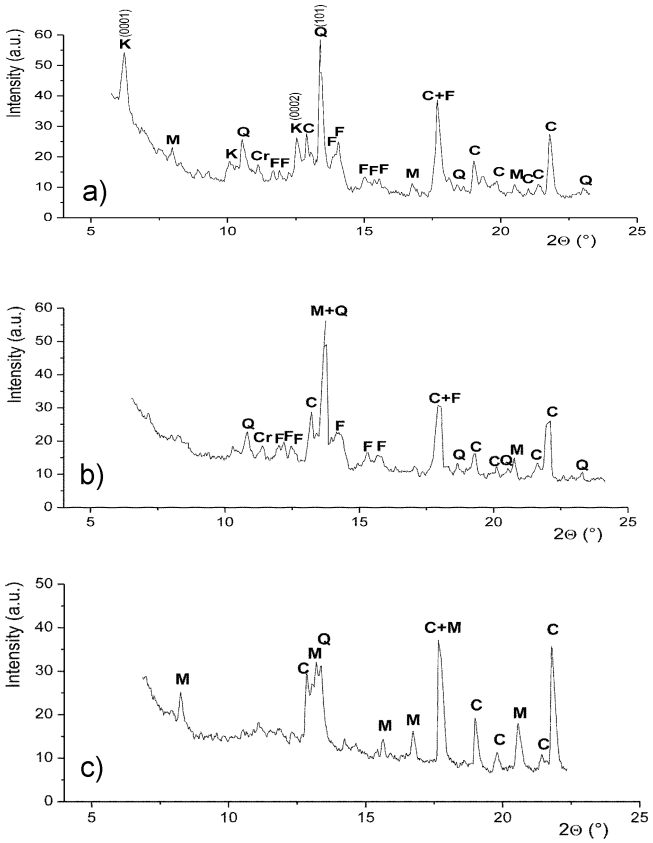


**Fig. 1** . X-ray diffraction pattern of a) as-received, b) dehydroxylated, and c) fired cold-isostatically pressed alumina-based electroporcelain (Q-quartz, K-kaolinite, Cr-cristobalite, F-feldspar, C-corundum, M-mullite).

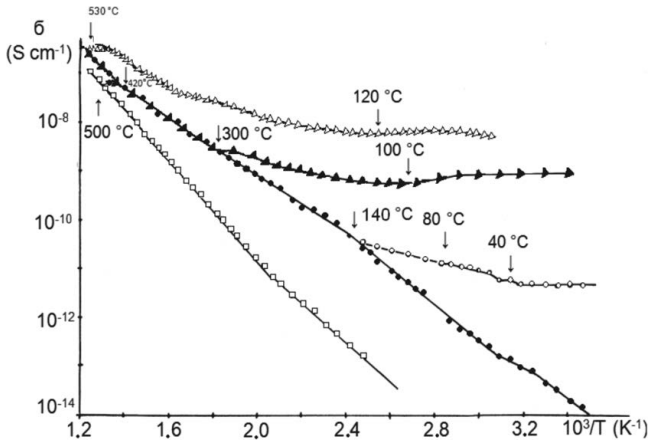


**Fig. 2** . Temperature dependences of dc and ac (1.6 kHz) conductivities for A and R samples, on different thermal processing: △ ac conductivity of as-received R samples, ▲ ac conductivity of R samples, on heating up to 530 °C, ■ ac conductivity of as-received A samples, ○ dc conductivity of "as-received" samples, • conductivity, on heating up to 160 °C, □ dc conductivity, on heating to 530 °C. (No difference between R- and A-samples is observed for the dc conductivity).

### *(2) Dc conductivity*

In cold-isostatically pressed electroporcelain, temperature dependences of the dc conductivity do not show any anisotropy in green (above 80 °C), dehydroxylated, or fired samples (Figs. 2,3). In as-received samples, the influence of release of the PBW on the dc conductivity is present up to 130 °C (Fig.2), resulting from a proton and $OH^-$ conduction which dominates at this temperature range[22–24]. On pre-heating up to 150 °C, temperature dependences of the dc conductivity, $\sigma_{dc}$, in both A-samples and R-samples, contain two sections given by two Arrhenius-like dependences,

$$\sigma_{dc} = \sigma_i \exp(-E_i/kT) \qquad (1)$$

where i = 1, 2; $\sigma_1$ and $E_1$ are the pre-exponential factor and conduction activation energy, respectively, of the high-temperature part (above 150 °C up to beginning of dehydroxylation); $\sigma_2$ and $E_2$ are the pre-exponential factor and conduction activation energy, respectively, of the low-temperature part (20–150 °C). All the parameters are, within error limits, the same for both A-samples and R-samples; $E_1$= 0.56 ± 0.02eV, $E_2$= 0.77 ± 0.02eV, $\sigma_1 = (4 \pm 1) \times 10^{-4}$ S/cm, $\sigma_2 = (5 \pm 1) \times 10^{-2}$ S/cm.

Upon starting the dehydroxylation process, at 420 °C or 410 °C for R-samples and A-samples, respectively, the dc conductivity decreases below the conductivity given by Eq.(1) (Fig.2). This process is completed at 500 °C or 460 °C for R-samples and A-samples, respectively.The dc conductivity of dehydroxylated samples is much lower than that of the green samples but its temperature dependence is also composed of two Arrhenius-like dependences (Eq.(1)). In dehydroxylated samples, parameters of the temperature dependences of the dc conductivity are as follows: up to 200–220 °C, $E_2 = 0.8 \pm 0.01$eV, $\sigma_2 = (1.7 \pm 0.5) \times 10^{-3}$ S/cm; above 220 °C, $E_1 = 1.07 \pm 0.03$eV, $\sigma_1 = 0.7 \pm 0.2$ S/cm. No difference is found between temperature dependences of the dc conductivity of dehydroxylated A-samples and R-samples, i.e. the cold-isostatically pressed dehydroxylated ceramics can be considered, from the point of view of the dc conductivity, as isotropic materials. After being subjected to the same thermal treatment, the conductivity of unfired cold isostatically pressed alumina-based electroporcelain is 1–2 orders of magnitude higher than that of unfired vacuum-extruded silica-based electroporcelain[6].

In Fig.3, temperature dependences of the dc conductivity, after successive pre-heating up to 20, 200, 300, 400, and 500 °C, are shown. On pre-heating at 250–450 °C, low-temperature parts of the dependences have the same value of conduction activation energies, 0.85 ± 0.02eV. At higher temperatures, these dependences merge into one common line with an activation energy of 0.56 ±0.02eV and pre-exponential factor of $(4 \pm 1) \times 10^{-4}$S/cm. This line is, within error limits, identical with the high-temperature part of the temperature dependence of the conductivity of as-received samples (Fig.2). In vacuum-extruded silica-based electroporcelain, this line is almost negligible (partial heating does not significantly influence the temperature dependence of the ionic conductivity)[6].

The dc conductivity of fired cold isostatically pressed alumina-based electroporcelain is isotropic. Its temperature dependence has an activation energy equal to 0.775 ± 0.005eV and the pre-exponential factor is equal to 13 ± 4S/cm, in the whole temperature range (Fig.4). Increasing the firing temperature does not change the electrical properties of fired ceramics; extending the firing time slightly enhances the dc conductivity.

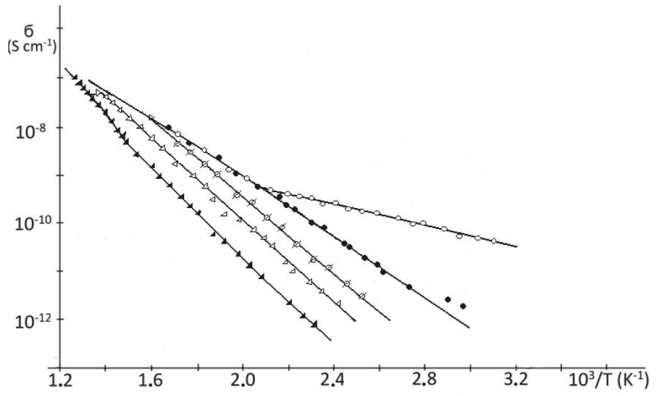


**Fig. 3:** Temperature dependences of the dc conductivity for cold-isostatically pressed alumina-based electroporcelain, on successive heating up to 20 (○), 200 (•), 300 (Ø), 400 (△), and 500 °C (△).

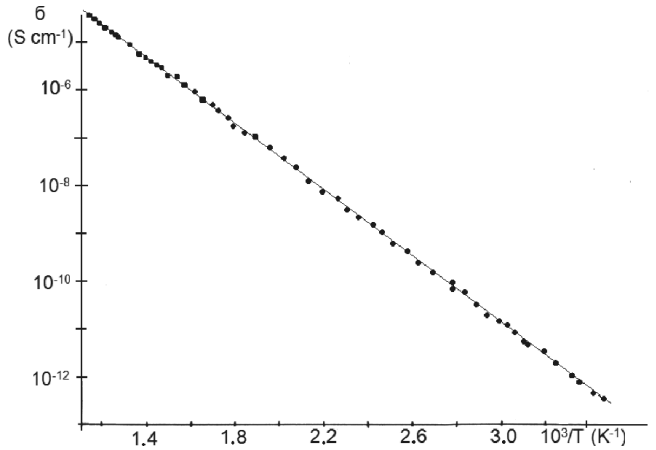


**Fig. 4:** Temperature dependence of the dc conductivity of fired, cold-isostatically pressed alumina-based electroporcelain. No anisotropy between R- (•••) and A- (■■■) samples is observed.

### *(3) Ac conductivity and effective permittivity*

In the temperature ranges of the release of both PBW and CBW, the anisotropy of the effective permittivity and ac conductivity is distinct in the as-received samples (Figs.5, 6). Both the ac conductivity ($\sigma_{ac}$) and the effective relative permittivity ($\varepsilon_r$) are higher in as-received R-samples up to 530 °C. In R-samples, minima of both $\sigma_{ac}$ and $\varepsilon_r$take place at 110 – 120 °C. At this temperature (for 1.6kHz), $\varepsilon_r$= 12.9, and the influence of an enhanced concentration of PBW and/or CBW on the $\sigma_{ac}$and $\varepsilon_r$is distinct up to 530 °C (Figs.5, 6). A-samples are already sufficiently dry at 110 °C, when $\varepsilon_r$= 6.3 (at 1.6kHz). Upon dehydroxylation, the static relative permittivity ($\varepsilon_{rs}$), of both A-samples and R-samples, is equal to 6.3 ± 0.3, at room temperature. Above 300 °C, the temperature dependences of both ac conductivity and dc conductivity of the dehydroxylated samples are very close to one another. Frequency dependences of the ac conductivity are given by a superposition of the dc conductivity and the frequency-dependent component with power-law behavior,

$$\sigma_{ac} = \sigma_{dc} + 9 \times 10^{-11} \int^{0,82} \qquad (2)$$

where *f* is the frequency in kHz and both conductivities are in S/cm.

Fired cold isostatically pressed alumina-based electroporcelain is not hygroscopic (traces of the PBW can be totally removed by brief heating to 150 °C). Their relative static permittivity at RT is equal to 6.9 ± 0.1, for both A- and R-samples. Effective relative permittivity, at 1.6kHz and RT, is equal to 7.2 ± 0.1. The ac and dc conductivities of the fired ceramics are identical.

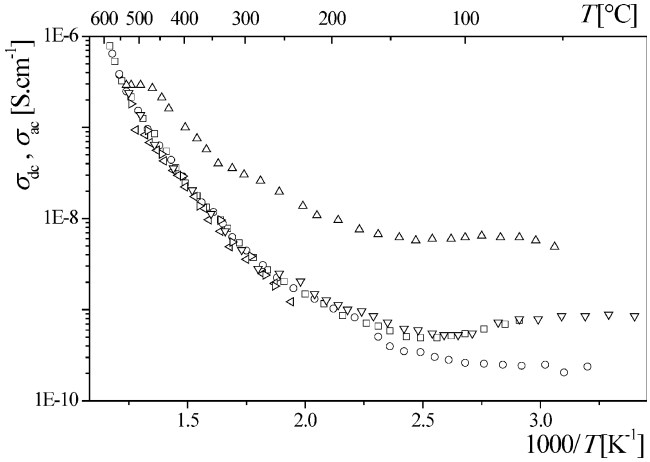


**Fig. 5:** Temperature dependences of the ac (1.6 kHz) and dc conductivities of cold-isostatically pressed alumina-based electroporcelain, on various thermal treatments – A samples: □□□ ac, 1st heating; ○○○ ac, 2nd heating, ◁◁◁ dc; R samples - △△△ ac, 1st heating; ▽ ▽ ▽ ac, 2nd heating, ▷▷▷ dc.

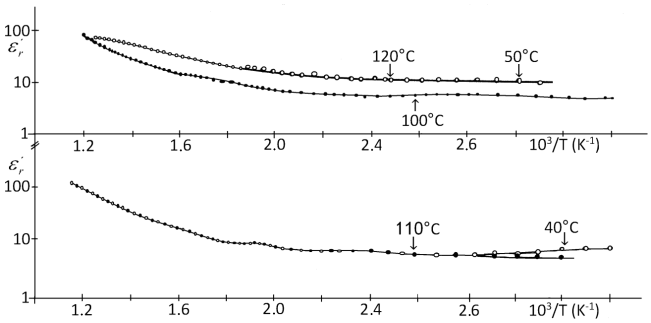


**Fig. 6:** Temperature dependence of the effective relative permittivity, at 1.6 kHz, of R (upper figure) and A (lower figure) samples from cold-isostatically pressed alumina-based electroporcelain; samples – as- received (○○○), on heating to 550 °C (•••).

## IV. Discussion

Dc conductivities of both silica-based and alumina-based green electroporcelain depend on the concentration and mobility of $H^+$, $Na^+$, $K^+$, and $OH^-$ ions[6, 22–24, 28]. Temperature dependences of the dc conductivity contain several Arrhenius-like sections. In as-received samples, protons and $OH^-$ ions are dominant charge carriers, up to 140 °C. The mobility of $Na^+$ or $K^+$ ions and their contribution to the dc conductivity are low in this temperature range. After pre-heating at 150 °C, a decrease of the dc conductivity and an increase of the conduction activation energy at low temperatures indicate a diminution of the proton and $OH^-$concentrations[22–24] and onset of a cooperative motion of $H^+$, $Na^+$, and $K^+$ ions. Above 140 °C, free $Na^+$ and $K^+$ ions are dominant charge carriers as they are sufficiently mobile at these higher temperatures. When the dehydroxylation process starts, the dc conductivity decreases below the values given by the Eq.(1). This process begins at a slightly higher temperature

in the R-samples. It means that the orientation of pores and capillaries is important not only for the rate of PBW release but also for that of CBW release[2]. During successive heating, temperature dependences of the dc conductivity (Fig.3) indicate a progressive decrease of free alkali ions due to their association with residual $OH^-$ ions into neutral $Na^+$-$OH^-$ or $K^+$-$OH^-$ complexes which do not contribute to the dc conductivity[25]. Because the concentration of free alkali ions along the "partial heating" conductivity dependence is constant (frozen at the value determined by the temperature of the partial annealing) the activation energy of 0.85eV determines the mobility activation enthalpy of alkali ions. The activation energy of the common line, 0.56 eV, is lowered due to the association energy of $Na^+$-$OH^-$ or $K^+$-$OH^-$ dipoles[25]. The identity of this line with the high-temperature part of the temperature dependence of the dc conductivity of as-received samples confirms that the heating rate of 2 °C/min is low enough to obtain the equilibrium concentration of mobile defects at all temperatures during measurements of temperature dependences. Owing to a removal of the CBW[26] and association of released $OH^-$ ions with mobile alkali metal ions, the process of dehydroxylation is accompanied by a temporary decrease of the dc conductivity. This behavior is also typical for a dehydroxylation of silica-based ceramics, kaolin, and illite[6, 27–31]. This decrease is not observed in temperature dependences of the ac conductivity (Fig.5). It results from the association of free $Na^+$or $K^+$ions with released $OH^-$ ions into neutral dipolar units, during dehydroxylation. These neutral dipolar units do not contribute to the dc conductivity; therefore, the dc conductivity temporarily decreases. However, they contribute to the ac conductivity through their dielectric relaxation; therefore, the ac conductivity continuously increases with increasing temperature[25]. Upon dehydroxylation, structural rearrangement causes an enhancement of the conduction activation energy for a long-distance dc transport and a large decrease of the dc conductivity.

Ac conductivity depends both on the mobility and dielectric relaxation of free monovalent ions and on the relaxation of neutral dipolar complexes of ions which do not contribute to long-distance migration.

Permittivity depends on the water content in electroporcelain because water has a very high relative permittivity (81.6).

A removal of the PBW is accompanied by a rapid decrease of $H^+$, $OH^-$, and $H_2O$ content in the samples[6,11]. It results in a decrease of both ac conductivity and permittivity of ceramics. As-received, cold isostatically pressed, green R-samples absorb the PBW more willingly than green A-samples[2,6]. Their ac conductivity and effective relative permittivity is higher than those of A-samples (Figs.5, 6). This fact is connected with preferential orientation of closed anisometric pores and capillaries also in isostatically pressed ceramics. In A-samples, the first stage of removal of the PBW is completed at the temperature of the minimum relative permittivity or ac conductivity (100 – 120 °C). However, in R-samples, a part of the PBW is captured in closed pores and capillaries and is pushed out from them only due to structural changes during the dehydroxylation process (Fig.6). This part of PBW results in an enhanced ac conductivity and effective permittivity, in as-received R-samples at temperatures up to 530 °C (Figs.5, 6). After pre-heating up to 150 °C (A-samples) or 530 °C (R-samples), the dc and ac conductivities are the same in the range of 300 – 450 °C (Figs.2, 5); it means that both conductivities are determined only by the mobility and concentration of free alkali ions. An increase of the effective permittivity with increasing temperature results from polarization phenomena at grain boundaries and electrodes[32,33].

Electrical conductivities of fired alumina-based and silica-based electroporcelain[6] are almost the same, although the composition and microstructure of their green bodies are quite different. It results from the fact that the conductivity in fired ceramics is determined by the glass phase, in which $Na^+$ and $K^+$ ions are dominant charge carriers[6].

Identical values of ac and dc conductivities confirm a disappearance of water and products of its hydrolysis in fired ceramics. Thus, the texture and the anisotropy of electrical properties disappears in fired ceramics. The unfavorable influence of the texture is important only during preparation of electroporcelains. Above 300 °C, both alumina-based and silica-based[6] fired electroporcelain can be considered fast ionic conductors.

## V. Conclusions

Cold-isostatically pressed alumina-based electroporcelain is, from the point of view of X-ray diffraction and dc conductivity, isotropic. However, owing to anisometry of pores and capillaries, the content of the PBW and the rate constant of release of both the PBW and CBW depend on the orientation of samples. As-received, cold isostatically pressed, green R-samples absorb the PBW more willingly than as-received green A-samples. Their ac conductivities and effective permittivities are higher than those of the A-samples. The process of PBW release from the R-samples is only completed at the onset of dehydroxylation. At pre-heating temperatures up to 150 °C, the dc conductivity, $\sigma_{dc}$, is isotropic and its temperature dependence is a superposition of two Arrhenius-like dependences (Eq. 1), where $E_1 = 0.56 \pm 0.02$eV, $E_2 = 0.77 \pm 0.02$eV, $\sigma_1 = (4 \pm 1) \times 10^{-4}$S/cm, $\sigma_2 = (5 \pm 1) \times 10^{-2}$S/cm. The ac conductivity and effective relative permittivity are anisotropic and higher in the R-samples. This anisotropy disappears after heating to 530 °C when the values of both variables of the R-samples drop to the values of the A-samples. The texture and the anisotropy of electrical properties disappear also in fired electroporcelain. It means that the unfavorable influence of the texture is important only during preparation of electroporcelains, e.g. on heating raw bodies.

Temperature dependences of the dc conductivity of the dehydroxylated samples are much lower than those of the green samples but they are also composed of two Arrhenius-like dependences (Eq. 1). Their parameters are as follows: up to 200 – 220 °C, $E_2 = 0.8 \pm 0.01$eV, $\sigma_2 = (1.7 \pm 0.5) \times 10^{-3}$S/cm; above 210 °C, $E_1 = 1.07 \pm 0.03$eV, $\sigma_1 = 0.7 \pm 0.2$S/cm. At room temperature, relative static permittivity is equal to $6.3 \pm 0.3$.

On firing at 1340 °C, temperature dependences of ac and dc conductivities are identical; they are Arrhenius-like throughout the whole temperature range, having the conduction activation energy equal to 0.775 ± 0.005eV, pre-exponential factor equal to 13 ± 4S/cm, and relative static permittivity at RT equal to 6.9 ± 0.1. Above 300 °C, the electrical conductivity of electroporcelain fired at 1340 °C is so high that the fired electroporcelain can be considered as a fast-ionic conductor. It has to be taken into account as from this porcelain the high-voltage insulators are produced.

## Acknowledgements

The work was supported by the Scientific Grant Agency VEGA, Slovak Republic – project No. 0162/15. The authors thank ceramic plant PPC Čab for providing the ceramics studied.

## References

[1] Hoffman, M., Danheim, H.: Development of technological texture in extruded ceramics, *Keramische Zeitschrift*, **39**, 86 – 91, (1987).

[2] Lučininova, N.I.: Investigation of texture of the ceramic blank by thermographic methods, *Steklo i keramika*, **12**, 16 – 18, (1979)

[3] Štubňa, I., Kalužná, M., Trnovcová, V.: Mapping the structure of electroporcelain blank by radiointroscopy, *Ind. Ceram.*, **30**, 17 – 20, (2010).

[4] Boatner, L.A., Bolduo, J.L., Abraham, M.M.: Characterization of textured ceramics by electron paramagnetic resonance spectroscopy, *J. Am. Ceram. Soc., 73, 2333 – 2335, (1990).*

[5] Kozík, T., Minárik, S.: New possibilities for investigation of the technological texture based on measurement of electric parameters: theoretical analysis and experimental verification, *J. Electr. Eng.*, **64**, 376 – 380, (2013).

[6] Trnovcová, V., Furár, I., Hanic, F.: Influence of technological texture on electrical properties of industrial ceramics, *J. Phys. Chem. Solids*, **68**, 1135 – 1139, (2007).

[7] Štubňa, I., Valovič, Š.: Thermal expansion of textured electroceramics, *Ind. Ceram.*, **24**, 121 – 124, (2004).

[8] Kalužná, M., Vozár, L., Gembarovič, J., Kaprálik,I.: The effect of texture on the thermal diffusivity of ceramic material, *Ceram.-Silikáty*, **36**, 15 – 19, (1992).

[9] Štubňa, I., Trnovcová, V.: The effect of texture on thermal expansion of extruded ceramics, *Ceram.-Silikáty*, **42**, 21 – 24, (1998).

[10] Štubňa, I., Lintnerová, A., Vozár, L.: Anisotropic mechanical properties of textured quartz porcelain, *Ceram.-Silikáty*, **52**, 90 – 94 (2008).

[11] Štubňa, I., Šín, P., Trník, A., Podoba, R., Vozár, L.: Development of Young's modulus of the green alumina porcelain raw mixture, *J. Aust. Ceram. Soc.* (in press)

[12] Šín, P., Podoba, R., Štubňa, I., Trník, A.: Mechanical properties of alumina porcelain during heating, *AIP Conf. Proc.*, 1634 – 76 – 80, (2014).

[13] Lerdprom, W., Li, C., Jayaseelan, D.D., Skinner, S.J., Lee, W.E.: Temperature dependence of electrical conductivity of a green porcelain mixture, *J. Eur. Ceram. Soc., 17, 343 – 349, (2017).*

[14] Lerdprom, W., Grasso, S., Jayaseelan, D.D., Reece, M.J., Lee, W.E.: Densification behavior and physico-mechanical properties of porcelains prepared using spark plasma sintering, *Adv. Appl. Ceram.*, **116**, 307 – 315, (2017).

[15] Lee, S.J., Kim, Y.J., Moon, H.S.: Energy-filtering electron microscopy (EF-TEM) study of a modulated structure in metakaolinite represented by a 14 Å modulation, *J. Am. Ceram. Soc., 86, 174 – 176, (2003).*

[16] Wang, X., Xiao, P.: Characterization of clay sintering process using impedance spectroscopy, *J. Eur. Ceram. Soc., 22, 471 – 478, (2002).*

[17] Lee, V.G., Yeh, T.H.: Sintering effects on the development of mechanical properties of fired clay ceramics, *Mater. Sci. Eng. A, 485, 5 – 13, (2008).*

[18] Sainz, M.A., Serrano, F.J., Amigo, J.M., Bastida, J., Caballero, A.: XRD microstructural analysis of mullites obtained from kaolinite-alumina mixtures, *J. Eur. Ceram. Soc., 20, 403 – 412 (2000).*

[19] Chakraborty, A.K.: DTA study of preheated kaolinite in the mullite formation region, *Thermochim. Acta*, **398**, 203 – 209, (2003).

[20] Cheng, Y.F., Wang, M.Ch., Hong, M.H.: Phase transformation and growth of mullite in kaolin ceramics, *J. Eur. Ceram. Soc., 24, 2389 – 2397, (2004).*

[21] Amigó, J.M., Serrano, F.J., Kojdecki, M.A., Bastida, J., Esteve, V., Reventós, M.M., Martí, F.: X-ray microstructure analysis of mullite, quartz and corundum in porcelain insulators, *J. Eur. Ceram. Soc., 25, 1479 – 1486, (2005).*

[22] Kubliha, M., Trnovcová, V., Ondruška, J., Štubňa, I., Bošák, O., Kaljuvee, T.: Comparison of dehydration in kaolin and illite using DC conductivity measurements, *Appl. Clay Sci.*, **149**, 8 – 12, (2017).

[23] Kubliha, M., Trnovcová, V., Ondruška, J., Štubňa, I., Bošák, O., Kaljuvee, T., Bačík, P.: DC conductivity of illitic clay after various firing, *J. Therm. Anal. Calorim.,* **124**, 81 – 86, (2016).

[24] Podoba, R., Štubňa, I., Trnovcová, V., Trník, A.: Temperature dependence of DC electrical conductivity of kaolin, *J. Therm. Anal. Calorim.,* **118**, 597 – 601, (2014).

[25] Hartmanová, M., Trnovcová, V.: Ionic crystals, Alfa, Bratislava 1972 (in Slovak).

[26] Heide, K., Foldvari, M.: High-temperature mass spectrometric gas-release studies of kaolinite $Al_2[Si_2O_5(OH)_4]$ decomposition, *Thermochim. Acta*, **446**, 106 – 112, (2006).

[27] Štubňa, I., Varga, G., Trník, A.: Investigation of kaolinite dehydroxylation is still interesting, *Építoanyag*, **58**, 6 – 9, (2006).

[28] Trnovcová, V., Podoba, R., Štubňa, I.: dc conductivity of kaolin-based ceramics in the temperature range 20 – 600 °C, *Építoanyag*, **64**, 46 – 49, (2012).

[29] Štubňa, I., Kozík, T.: Electrical conductivity of kaolin in the temperature range 150 – 560 °C, *J. Thermal Anal.*, **46**, 607 – 610, (1996).

[30] Kozík, T., Trnovcová, V., Mariani, E., Štubňa, I., Roháč, J.: The temperature dependence of the electrical conductivity of unfired porcelain mixture, *Ceram.-Silikáty*, **36**, 69 – 72, (1992).

[31] Trnovcová, V., Kozík, T., Mariani, E., Štubňa, I.: Relaxation of electrical properties of electroporcelain compacts over the temperature range 20 – 250 °C, *Ceram.-Silikáty*, **32**, 233 – 240, (1988).

[32] Ondruška, J., Štubňa, I., Trnovcová, V., Vozár, L., Bačík, P.: Polarization currents in illite at various temperatures, *Appl. Clay Sci.*, **135**, 414 – 417, (2017).

[33] Ondruška, J., Štubňa, I., Trnovcová, V., Medveď, V., Kaljuvee, T.: Polarization and depolarization currents in kaolin, *Appl. Clay Sci.*, **114**, 157 – 160, (2015).